Security-Constrained Temperature-Dependent Optimal Power Flow Using Hybrid Pseudo-Gradient based Particle Swarm Optimization and Differential Evolution

Minh-Trung Dao[1,2], Khoa Hoang Truong[3,4,*], Duy-Phuong N. Do[2], Bao-Huy Truong[5], Khai Phuc Nguyen[1,4], and Dieu Ngoc Vo[1,4]

[1]Department of Power Systems, Ho Chi Minh City University of Technology (HCMUT), 268 Ly Thuong Kiet Street, District 10, Ho Chi Minh City, Vietnam
[2]Department of Electrical Engineering, College of Engineering Technology, Can Tho University, Can Tho City, Vietnam
[3]Department of Power Delivery, Ho Chi Minh City University of Technology (HCMUT), 268 Ly Thuong Kiet Street, District 10, Ho Chi Minh City, Vietnam
[4]Vietnam National University Ho Chi Minh City, Linh Trung Ward, Thu Duc City, Ho Chi Minh City, Vietnam
[5]Institute of Engineering and Technology, Thu Dau Mot University, Binh Duong Province, Viet Nam
*Corresponding author: Email: trhkhoa@hcmut.edu.vn

Abstract: Conventional optimal power flow studies neglect the effect of temperature on resistance for simple calculation. However, the branch resistance changes with the change of temperature. Thus, the optimal power flow (OPF) should consider the temperature effect for accurate calculation. Moreover, contingency cases should be considered to ensure system security. Accordingly, the security-constrained temperature-dependent optimal power flow (SC-TDOPF) emerges as a critical and practical issue in power systems. To deal with the SC-TDOPF problem, this study suggests a hybrid method, namely pseudo-gradient based particle swarm optimization and differential evolution method (PGPSO-DE). The suggested PGPSO-DE method is applied to the standard IEEE 30 bus system under normal condition as well as contingency condition. The findings have shown that the PGPSO-DE method provides better solution quality than other studied optimization methods. Consequently, the PGPSO-DE method proves its effectiveness in solving the complex SC-TDOPF problem.

Keywords: Power flow analysis; security-constrained; temperature-dependent power flow (TDPF); differential evolution; particle swarm optimization; optimal power flow; pseudo gradient; hybrid method.

1. Introduction

Power flow is always performed to calculate the fitness function when solving the important optimization problems in power systems such as economic dispatch, unit commitment, optimal power flow, optimal reactive power dispatch, and hydrothermal scheduling. Power flow analysis is also used to perform the contingency analysis and transient stability study. Therefore, the accuracy of power flow study is a very essential concern. In conventional power flow calculation, the temperature effect is ignored and the resistance of the elements of power systems is treated as a constant. However, the resistance is a function of temperature. As the temperature rises, the resistance of a metallic conductor rises as well. Therefore, there is always an error related to temperature in conventional power flow and branch loss calculation. To obtain more accurate results, power flow calculation should consider the temperature effect. This study investigates the optimal power flow (OPF) problem considering the temperature effect. A fully coupled temperature-dependent power flow (TDPF) algorithm in [1] is used for power flow calculation in this study.

The OPF problem is one of the most important tools in power system operation and planning. Its solution offers the optimal settings for generators, transformers, and shunt capacitors which

Received: October 8th, 2022. Accepted: March 23rd, 2023
DOI: 10.15676/ijeei.2023.15.1.6

minimize the considered objective function (e.g., total fuel cost) while satisfying various system operating limits [2]. The OPF problem has a long history of development since it was first introduced in 1962 [3]. This problem has been initially solved by traditional methods based on mathematical programming such as Newton-based techniques [4], linear programming [5], non-linear programming [6], quadratic programming [7], and interior point methods [8]. In general, these methods have short computational time and effectively solve the simple OPF problem with convex and continuous objective functions. However, the practical OPF is a large-scale, non-linear and non-convex optimization problem. This is a challenge for solution methods, especially for the traditional methods. They may suffer difficulty in finding a global solution or cannot successfully solve the complex OPF problem. To overcome these barriers, advanced optimization methods (i.e., meta-heuristic methods) have been developed based on biological simulation to cope with the complex OPF problem. The meta-heuristic methods have the advantage of obtaining near-optimum solutions for any type of optimization problem. Therefore, these methods have been widely implemented to various engineering fields. For the OPF problem, the meta-heuristic methods have also been successfully solved this problem such as genetic algorithm (GA) [9], particle swarm optimization (PSO) [10], differential evolution (DE) [11], artificial bee colony (ABC) algorithm [12], biogeography-based optimization (BBO) [13], grey wolf optimizer (GWO) [14], moth swarm algorithm (MSA) [15], krill herd algorithm (KHA) [16], and moth-flame optimization (MFO) [17], etc. These methods have shown their effectiveness in dealing with this problem. However, they can consume long computational time and still suffer sub-optimal solutions when facing complicated and large-scale problems. Besides single methods, hybrid methods based on the combination of different algorithms have been also developed to efficiently solve the complex OPF problem. Some hybrid methods are mentioned such as a hybrid of shuffle frog leaping algorithm (SFLA) and simulated annealing (SA) algorithm (SFLA-SA) [18], a hybrid method of modified imperialist competitive algorithm (MICA) and teaching learning algorithm (TLA) (MICA-TLA) [19], and a hybrid of particle swarm optimization (PSO) and gravitational search algorithm (GSA) (PSOGSA) [20]. In general, hybrid methods have the advantage of achieving high-quality solutions for complicated optimization problems. However, their disadvantage lies in the setting of many control parameters from the combined methods. Improper setting of control parameters can lead the algorithm not converge to the global solution.

The primary OPF problem was formulated under normal operating conditions of the power system. However, contingency cases (*e.g.*, outage of a transmission line) may occur. In such a situation, the solution from the OPF problem can violate the system operating constraints. Therefore, system security should be considered for the OPF problem to ensure the reliability and economic operation of power systems. In this context, the conventional OPF problem becomes a security-constraint OPF (SC-OPF) problem. By adding the security constraints, the solution of the SC-OPF problem is not only feasible for the normal case (N - 0) but also for the contingency case (N - 1). However, the problem becomes very complex and a great challenge for solution methods. Recently, many solution methods have been suggested for dealing with the SC-OPF problem. The study [21] proposed a modified bacteria foraging optimization algorithm (MBFA) to optimally operate the wind-thermal generation system with minimum cost reduction of the system loss while satisfying a voltage secure operation. Although a detailed cost model was introduced, the valve loading effects was not included in the cost model. In [22], a contingency partitioning approach was proposed for the preventive-corrective SC-OPF problem. The authors used a DC network model for calculation and the valve point loading effects was not considered in this study. A fuzzy based harmony search algorithm (FHSA) was suggested in [23] to determine the best solution for the SC-OPF problem. The objective function in this study was a quadratic fuel cost function, without considering the valve point loading effects of thermal generating units. In [24], an adaptive flower pollination algorithm (APFPA) was successfully solved the SCOPF problem with the different objective functions of minimizing the fuel cost, power losses and voltage deviation. A cross-entropy (CE) method in [25] was introduced to assess the SCOPF solutions. The corresponding SC-OPF stochastic problem was first defined,

and the CE was then applied to solve the formulated problem. The results obtained from the CE method for the IEEE 57 bus and IEEE 3000 bus systems showed that this method offered betters solutions with fewer evaluations than other compared algorithms. Moreover, the SC-OPF problem has been also solved by a hybrid method such as a hybrid canonical differential evolutionary particle swarm optimization (hC-DEEPSO) [26]. This hybrid method was tested on the IEEE standard systems including 57, 118, and 300 buses, showing its effectiveness from the comparison of obtained results with other evolutionary methods. In general, the SC-OPF problem is a highly nonlinear and non-convex optimization problem, posing a great challenge for finding a globally optimal solution.

In literature, regarding the OPF problem with temperature effect, there is a few studies have investigated this problem. In [27], the authors proposed a gbest-guided artificial bee colony (GABC) algorithm to solve the OPF problem as well as the temperature-dependent OPF (TDOPF) problem. Also, the TDOPF problem was solved by the chaotic whale optimization algorithm (CWOA) [28]. Both GABC and CWOA were tested on the IEEE 30 bus system, the 2383 bus winter peak Polish system, and the 2736 bus summer peak Polish system. However, these two studies did not consider the valve point loading effects in the objective function as well as the security constraint in the problem formulation. In this study, the OPF problem is investigated with the temperature effect. In addition, the valve point loading effects and the security constraint are also considered for the OPF problem. The new OPF problem is called the security constraint temperature-dependent OPF (SC-TDOPF) problem. To solve the SC-TDOPF problem, this study proposes a hybrid pseudo-gradient particle swarm optimization and differential evolution method (PGPSO-DE) [29]. The proposed PGPSO-DE method utilizes the search ability of PGPSO and DE to find the near-optimum solution. The PGPSO is used to explore the global search while the DE method is used to exploit the local search. As a result, the PGPSO-DE method has a key advantage of balance between exploration and exploitation. PGPSO-DE can deal with optimization problems having many control variables and complicated constraints such as the SC-TDOPF problem. The proposed method has been tested on the IEEE 30-bus system and their obtained results have been compared with other optimization methods.

2. Mathematical problem formulation of TDPF

The resistance of a metallic conductor increases as temperature increases. Thus, the resistance is proportional to the temperature and expressed as follows [1]:

$$R = R_{Ref} \times \frac{T + T_F}{T_{Ref} + T_F} \tag{1}$$

where R is the conductor resistance; R_{Ref} is the conductor resistance at the reference temperature; T is the conductor temperature; T_{Ref} is the reference temperature; and T_F is the temperature constant depending on the conductor metal.

A. Thermal model of elements in power systems

The thermal characteristic of the devices in power systems is modelled by a generalized thermal resistance model as shown in Figure 1.

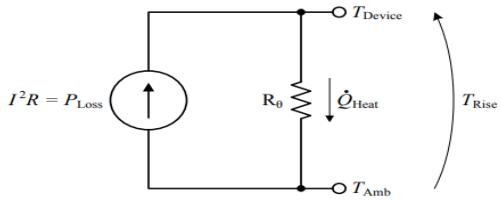

Figure 1. Thermal resistance model for branch element in power system.

In a thermal resistance model, the device temperature rise of the device is linearly proportional to the loss of the device. The ratio between the steady-state temperature rise and the loss of that device is the thermal resistance.

$$R_\theta = \frac{T_{Rise}}{P_{Loss}} = \frac{T_{RatedRise}}{P_{RatedLoss}} \tag{2}$$

where, R_θ is the thermal resistance; T_{Rise} is the device temperature rise above ambient; P_{Loss} is the power loss within the device; $T_{RatedRise}$ is the rated (or reference) device temperature rise; and $P_{RatedLoss}$ is the corresponding rated (or reference) loss.

The temperature of the device (T) equals the ambient temperature (T_{Amp}) plus the device temperature rise above ambient (T_{Rise}). Rearranging Eq. (2), the temperature of the device is expressed as follows:

$$T = T_{Amp} + \left(\frac{P_{Loss}}{P_{RatedLoss}} \right) T_{RatedRise} \tag{3}$$

If P_{Loss} is suitably expressed as a function of voltage and temperature state, Eq. (3) can be directly used in power flow calculation.

Besides the thermal model of branch element, the other thermal models of power system elements such as overhead lines, underground cables, and transformers are given in [1].

B. Equations of TDPF problem

In the TDPF problem, it is assumed that the system must operate in both thermal and steady-state cases. In addition, there are three main modifications to the conventional power flow as follows [1]:

B.1. State Vector:

Besides the conventional state variables like V and δ, an additional state variable T for the temperature is considered for each temperature-dependent branch. Accordingly, the state vector has the form:

$$x = \begin{bmatrix} V \\ \delta \\ T \end{bmatrix} \tag{4}$$

in which, all state variables are expressed in per-unit.

B.2. Mismatch Equations:

Conventional power flow employs two mismatch equations including real and reactive power mismatch equations. The TDPF problem requires two those convention mismatch equations and an additional mismatch equation of temperature difference. Three mismatch equations of the TDPF are described as follows:

$$\Delta P_i = (P_{Gen,i} - P_{Load,i}) - P_i(\delta, V, T) \tag{5}$$

$$\Delta Q_i = (Q_{Gen,i} - Q_{Load,i}) - Q_i(\delta, V, T) \tag{6}$$

$$\Delta H_{ij} = 0 - H_{ij}(\delta, V, T) \tag{7}$$

B.3. Jacobian Matrix

The Jacobian matrix must be restructured due to the addition of the state variable T. Partial derivatives of real power, reactive power and temperature difference equation are taken with respect to each variable in the state vector (δ, V, and T). The restructured Jacobian matrix is expressed as follows:

$$J(\delta,V,T)=\begin{bmatrix}\frac{\partial P}{\partial \delta} & \frac{\partial P}{\partial V} & \frac{\partial P}{\partial T}\\ \frac{\partial Q}{\partial \delta} & \frac{\partial Q}{\partial V} & \frac{\partial Q}{\partial T}\\ \frac{\partial H}{\partial \delta} & \frac{\partial H}{\partial V} & \frac{\partial H}{\partial T}\end{bmatrix} \tag{8}$$

B.4. Overall procedure of Fully Coupled TDPF

There are four types of TDPF as described in [1]. This paper employs fully coupled TDPF (FC-TDPF) for calculation. If the Jacobian matrix in Eq. (8) is used, the overall procedure of FC-TDPF is described as follows:

Step 1: Initialize all state variables (*ie.*, δ, V, and T).
Step 2: Update all branch resistances according to the most recent temperature. Calculate the admittance matrix Y_{bus}.
Step 3: Calculate the Jacobian matrix as in Eq. (8).
Step 4: Calculate the mismatch (*ie.*, ΔP, ΔQ, and ΔH) using Eqs. (5-7)
Step 5: Update δ, V, and T as follows:

$$\begin{bmatrix}\delta^{v+1}\\ V^{v+1}\\ T^{v+1}\end{bmatrix}=\begin{bmatrix}\delta^{v}\\ V^{v}\\ T^{v}\end{bmatrix}-J(\delta^{v},V^{v},T^{v})^{-1}.\begin{bmatrix}\Delta P^{v}\\ \Delta Q^{v}\\ \Delta H^{v}\end{bmatrix} \tag{9}$$

Step 6: If ΔP, ΔQ, $\Delta H < \varepsilon$ (ε is the specified tolerance), stop the loop. Otherwise, go to Step 2.

3. Problem formulation

The SC-TDOPF is a very complicated optimization problem. This problem has many control variables and complex constraints that need to be handled. The goal of this problem is to determine an optimal set of control variables so as the total cost of thermal generating units is minimized while satisfying various constraints of the system in both normal and contingency cases. In general, the SC-TDOPF problem is mathematically formulated as follows:

$$\text{Minimize } F(U,X) \tag{10}$$

subject to the following constraints for the normal case:

$$h(U,X)=0 \tag{11}$$

$$g(U,X)\le 0 \tag{12}$$

and the following constraints for the contingency cases:

$$h(U^{S},X^{S})=0 \tag{13}$$

$$g(U^{S},X^{S})\le 0 \tag{14}$$

where $F(.)$ represents the fuel cost function of generators, U and X are the set of state and control variables, respectively; $h(.)$ and $g(.)$ are the set of the equality and inequality constraints, respectively; and S is the set of outage lines.

A. Objective function

The objective function is to minimize the total fuel cost of all thermal generating units.

$$\text{Min } F = \text{Min}\sum_{i=1}^{N_g} F_i(P_{gi}) \tag{15}$$

where N_g is the total number of thermal units; and P_{gi} is the power output of thermal unit i

In Eq. (15), a quadratic function is used to expressed the fuel cost function of a thermal generating unit i as follows:

$$F_i(P_{gi}) = a_i + b_i P_{gi} + c_i P_{gi}^2 \tag{16}$$

The solution of the SC-TDOPF is more accurate and practical when considering the valve point effects (VPEs) of thermal generating units. As a result, the fuel cost function is represented as a quadratic function adding a sinusoidal function:

$$F_i(P_{gi}) = a_i + b_i P_{gi} + c_i P_{gi}^2 + \left| e_i \sin(f_i(P_{gi,\min} - P_{gi})) \right| \quad (17)$$

where a_i, b_i, c_i, e_i and f_i are fuel cost coefficients N_g is the total number of generators; and $P_{gi,min}$ is the minimum power output of generator i.

B. System Constraints

For both normal and contingency cases, the objective function of the SC-TDOPF problem is subject to the following constraints:

i. Equality constraints:

$$P_{gi} - P_{di} = V_i \sum_{j=1}^{N_b} V_j \left(G_{ij}(T) \times \cos(\delta_i - \delta_j) + B_{ij}(T) \times \sin(\delta_i - \delta_j) \right) \quad \text{i = 1, 2, …, N}_\text{b} \quad (18)$$

$$Q_{gi} - Q_{di} = V_i \sum_{j=1}^{N_b} V_j \left(G_{ij}(T) \times \sin(\delta_i - \delta_j) - B_{ij}(T) \times \cos(\delta_i - \delta_j) \right) \quad \text{i = 1, 2, …, N}_\text{b} \quad (19)$$

$$T_{ij} - \left(T_{Amp} + R_{\theta,ij} \left(g_{ij}(T) \times (V_i^2 + V_j^2) - 2 g_{ij}(T) \times V_i V_j \cos(\delta_i - \delta_j) \right) \right) = 0 \quad \text{i = 1, 2, …, N}_\text{b} \quad (20)$$

where Q_{gi} is the reactive power outputs of generator i; V_i and δ_i are the magnitude and angle of voltage at bus i, respectively; V_j and δ_j are the magnitude and angle of voltage at bus j, respectively; P_{di} and Q_{di} are the active and reactive power demands at load bus i, respectively; G_{ij} and B_{ij} are the real and imaginary components of elements in the admittance matrix; g_{ij} is the conductance of line ij; and N_b is the number of buses in the system.

ii. Power generation output limits:

$$P_{gi,\min} \le P_{gi} \le P_{gi,\max} \quad i = 1, 2, \ldots, N_g \quad (21)$$

$$Q_{gi,\min} \le Q_{gi} \le Q_{gi,\max} \quad i = 1, 2, \ldots, N_g \quad (22)$$

where $P_{gi,min}$ and $P_{gi,max}$ denote the limits of active power outputs while $Q_{gi,min}$ and $Q_{gi,max}$ denote the limits of reactive power outputs of generator i.

iii. Bus voltage limits:

$$V_{gi,\min} \le V_{gi} \le V_{gi,\max} \quad i = 1, 2, \ldots, N_g \quad (23)$$

$$V_{li,\min} \le V_{li} \le V_{li,\max} \quad i = 1, 2, \ldots, N_d \quad (24)$$

where V_{gi} and V_{li} are the voltage magnitude at generation bus i and load bus i, respectively; $V_{gi,max}$ and $V_{gi,min}$ represent the limits of voltage magnitudes at generation bus i; $V_{li,max}$ and $V_{li,min}$ present the limits of voltages at load bus i; and N_d is the number of load buses.

iv. Shunt VAR compensator limits:

$$Q_{ci,\min} \le Q_{ci} \le Q_{ci,\max} \quad i = 1, 2, \ldots, N_c \quad (25)$$

where Q_{ci} is the shunt VAR compensation at bus i; $Q_{ci,max}$ and $Q_{ci,min}$ denote the capacity limits of shunt VAR compensator; and N_c is the number shunt VAR compensator.

Transformer tap settings limits:

$$T_{k,\min} \le T_k \le T_{k,\max} \quad k = 1, 2, \ldots, N_t \quad (26)$$

where; $T_{k,min}$ and $T_{k,max}$ present the limits of tap settings of transformer k; T_k is the value of tap setting of transformer k; and N_t is the number of transformer tap settings.

v. Transmission line limits

$$S_l \le S_{l,\max} \quad l = 1, 2, \ldots, N_l \tag{27}$$

where S_l and $S_{l,max}$ are the apparent power flow and the rating of transmisson line l, respectively; and N_l is the number of transmission lines.

For the security constraint, the values of the severity index (SI) are calculated to rank the severe cases of line outage as follows:

$$SI = \sum_{l=1}^{N_l} \left(\frac{S_l}{S_{l,\max}} \right)^2 \quad l = 1, 2, \ldots, N_l \tag{28}$$

4. The hybrid PGPSO and DE method

A. Pseudo-Gradient Particle Swarm Optimization Method

PSO is a well-known meta-heuristic optimization method. This method simulates the behaviors of birds or fishes in finding their food [30]. The PSO method is widely implemented to various optimization problems due to its simple structure and it is applicable to large-scale problems. PSO initializes randomly a population (swarm) containing individuals (particles). Each particle has a position vector X_i and a velocity vector V_i, indicating that each particle has a specific velocity for moving from its position to another.

Mathematically, the position of each particle d is expressed as follows:

$$V_{id}^{(n+1)} = \omega \times V_{id}^{(n)} + c_1 \times rand_3 \times (Pbest_d - X_{id}^{(n)}) + c_2 \times rand_4 \times (Gbest - X_{id}^{(n)}) \tag{29}$$

and the corresponding velocity of this particle is updated by:

$$X_{id}^{(n+1)} = X_{id}^{(n)} + V_{id}^{(n)} \tag{30}$$

where c_1 is the coefficient of the individual cognitive component and c_2 is the coefficient of the social cognitive component; ω is the inertia weight parameter; $Pbest_d$ is the best position of particle d at iteration n, and $Gbest$ is the best position in the population.

To enhance the search ability of PSO, Clerc and Kennedy introduced a constriction factor. [31]. The velocity for particles is modified as follows:

$$V_{id}^{(n+1)} = \chi(\omega \times V_{id}^{(n)} + c_1 \times rand_3 \times (Pbest_d - X_{id}^{(n)}) + c_2 \times rand_4 \times (Gbest - X_{id}^{(n)})) \tag{31}$$

where χ is the constriction factor and is determined as follows:

$$\chi = \frac{2}{\left| 2 - \varphi - \sqrt{\varphi^2 - 4\varphi} \right|}; \varphi = c_1 + c_2, \varphi > 4 \tag{32}$$

Besides the modification of the particle's velocity, the particle's position is updated by using the concept of pseudo-gradient [32]. In non-differentiable problems, the pseudo-gradient is used to determine whether the current particle's direction in the search space is good or not. Suppose that a particle moves from a point x_k to another x_l, the pseudo-gradient $g_p(x)$ is determined by the following rules [33]:

i. If $f(x_k) \ge f(x_l)$: The particle's direction is good, and the particle should keep moving in that direction. As a result, at point l, the pseudo-gradient is nonzero, (*i.e.,* $g_p(x_l) \neq 0$).

ii. If $f(x_k) < f(x_l)$: The particle's direction is not good, and the particle should move in a different direction. As a result, at point l, the pseudo-gradient is zero, (*i.e.,* $g_p(x_l) = 0$).

The rules above are used to update the new position of each particle as follows:

$$X_{id}^{(n+1)} = \begin{cases} X_{id}^{(n)} + g_p(X_{id}^{(n+1)}) \times |V_{id}^{(n+1)}| & \text{if } g_p(X_{id}^{(n)+1}) \neq 0 \\ X_{id}^{(n-1)} + V_{id}^{(n)+1} & \text{otherwise} \end{cases} \tag{33}$$

This study uses the pseudo-gradient guided PSO (PGPSO) method for the suggested hybrid approach.

B. Differential Evolution Method

Differential evolution (DE) is also a well-known meta-heuristic optimization method used for solving complex optimization problems. DE also initializes with a random population. A new population is created via three main stages as follows [34]:

- *Mutation stage*: In this stage, a new individual is generated based on other random individuals as in Eq (34). Thus, the search space of the problem is effectively explored.

$$X_{id}^{'(n)} = X_{r1d}^{(n)} + F \times (X_{r2d}^{(n)} - X_{r3d}^{(n)}) \tag{34}$$

where, $X_{id}^{'(n)}$ is the newly created individuals; *r1*, *r2*, and *r3* are random indexes of the population; and *F* is the mutation factor selected in [0,1].

- *Crossover stage:* To increase the diversity, this stage mixes the mutant vector $X_{id}^{'(n)}$ and the current solution $X_{id}^{(n)}$ to create a trial individual $X_{id}^{''(n)}$:

$$X_{id}^{''(n)} = \begin{cases} X_{id}^{'(n)} & \text{if } rand_5 \le CR \text{ or } d = D_{rand} \\ X_{id}^{(n)} & otherwise \end{cases} \tag{35}$$

where *CR* is the crossover rate in [0,1]; and D_{rand} is a random index of the population.

- *Selection stage:* The fitness values are computed for the current and trial individuals. The individual with a better fitness value is chosen for the next generation. In this way, a new generation has better individuals than the previous one.

C. The Hybrid PGPSO and DE Method

In general, PGPSO and DE have their advantages and disadvantages when dealing with different optimization problems. PGPSO is capable of finding the near-optimal solution in a short time for a considered problem, however, it is not guaranteed to provide high solution quality for complex problems. On the contrary, DE can easily find a high-quality solution for small-scale problems but may not be able to solve large-scale ones. In other words, it can be said that PGPSO has the advantage of good exploration while DE has the advantage of good exploitation. Therefore, this study proposes a combination of PGPSO and DE to form a hybrid method. The hybrid PGPSO-DE method utilizes the advantages of PGPSO and DE to become an effective method to solve complicated optimization problems. The following are the main steps of the proposed methods:

- *Initialization:* Like other meta-heuristic methods, PGPSO-DE randomly initializes a population of *Np* individuals in their boundaries.
- *Creating the first new generation:* Based on the initialized generation, the mechanism of PGPSO is used to create the first new generation. The fitness values are calculated for newly generated individuals. The individual with the best fitness value is selected for the next generation.
- *Creating the second new generation:* In this step, the DE method is used to create the second new generation. The new individuals are also evaluated via the fitness values to choose the best one for the next iteration.

5. Implementation of PGPSO-DE to the SC-TDOPF problem

This section describes the implementation of PGPSO-DE to the SC-TDOPF problem for the objective of minimizing the total fuel cost.

A. Initialization of Population

In the SC-TDOPF problem, there are two types of variables including control and state variables. In the population of PGPSO-DE, each individual includes the control variables described by a vector below:

$$X_{id} = [P_{g2}, P_{g3}, ..., P_{gN_g}, V_{g1}, V_{g2}, ..., V_{gN_g}, Q_{c1}, Q_{c2}, ..., Q_{N_c}, T_1, T_2, ..., T_{N_t}] \tag{36}$$

where P_{g1} is the real power output of the generator at the slack bus; $i = 1, 2, \ldots, N$ with $N = 2N_g + N_c + N_d - 1$ and $d = 1, 2, \ldots, N_p$ with N_p is the number of individual in the population.
Also, the state variables are represented as in Eq. (37).

$$U = [P_{g1}, Q_{g1}, Q_{g2}, ..., Q_{gN_g}, V_{l1}, V_{l2}, ..., V_{lN_d}, S_{l1}, S_{l2}, ..., S_{lN_l}] \tag{37}$$

The position and velocity of each individual are initialized as in Eq. (38) and Eq. (39), respectively.

$$X_{id}^{(0)} = X_{id}^{\min} + rand_1 \times (X_{id}^{\max} - X_{id}^{\min}) \tag{38}$$

$$V_{id}^{(0)} = V_{id}^{\min} + rand_2 \times (V_{id}^{\max} - V_{id}^{\min}) \tag{39}$$

where $X_{id}^{\max}$ and $X_{id}^{\min}$ are the maximum and minimum values for individual d, respectively; $V_{id}^{\max}$ and $V_{id}^{\min}$ denote velocity limits for individual d, respectively, which are calculated by:

$$V_{id}^{\max} = R \times (X_{id}^{\max} - X_{id}^{\min}) \tag{40}$$

$$V_{id}^{\min} = -V_{id}^{\max} \tag{41}$$

where R is the scale factor for the velocity.

B. Fitness function

Initial population and next created populations are used to solve the power flow problem to evaluate the quality of individuals. The fitness value is calculated for each individual via a fitness function in the normal case as follows:

$$FT_d^{(0)} = \sum_{i=1}^{N_g} F_i(P_{gi}) + K_{p0} \times (P_{g1} - P_{g1}^{\lim})^2 + K_{q0} \times \sum_{i=1}^{N_g} (Q_{gi} - Q_{gi}^{\lim})^2 + K_{v0} \times \sum_{i=1}^{N_d} (V_{li} - V_{li}^{\lim})^2 + K_{s0} \times \sum_{l=1}^{N_l} (S_l - S_{l,\max})^2 \tag{42}$$

where K_{p0}, K_{q0}, K_{v0}, and K_{s0} are the penalty factors for the normal case.

For the contingency case, the fitness function is calculated by:

$$FT_{d\_outage}^{(0)} = FT_d^{(0)} + K_q \times \sum_{i=1}^{N_g} (Q_{gi}^s - Q_{gi}^{\lim})^2 + K_v \times \sum_{i=1}^{N_d} (V_{li}^s - V_{li}^{\lim})^2 + K_s \times \sum_{l=1}^{N_l} (S_l^s - S_{l,\max})^2 \tag{43}$$

where, K_q, K_v, and K_s are the penalty factors for the outage case, Q_{gi}^s is the reactive power output of generator i in the contingency case; V_{li}^s is the voltage at load bus i in the contingency case; S_l^s is the apparent power flow in transmission line l in the contingency case.

In Eq. (42-43), the limitations of state variables are handled by:

$$X^{\lim} = \begin{cases} X_{\max} & \text{if } X > X_{\max} \\ X_{\min} & \text{if } X < X_{\min} \\ X & \text{otherwise} \end{cases} \tag{44}$$

Where X^{lim} denotes $P_{g1}^{\lim}$, $Q_{gi}^{\lim}$, $V_{li}^{\lim}$, and $S_{li}^{\lim}$ while X denotes P_{g1}, Q_{gi}, V_{li}, and S_{li}.

C. Overall procedure

The overall procedure for the implementation of the proposed PGPSO-DE method to solve the SC-TDOPF problem are described by the following steps:

Step 1: Set PGPSO-DE parameters: N_p, $Iter_{max}$, c_1 and c_2, R, F, and CR.
Perform the contingency analysis to obtain the SI values corresponding to each branch. Select the outage lines corresponding to the highest SI values.

Step 2: Initialize a random population as described in Section 5.1.

Step 3: Solve the power flow and calculate the fitness value for each individual in the initial population using Eq. (42). The position of the individual having the best fitness value is

set to *Gbest*. The initial population and the corresponding fitness function are set to $Pbest_d$ and FT_d^{best}, respectively. Set $k = 1$, k is the iteration counter.

Step 4: In this step, the mechanism of the PGPSO method is used to create the first new population. The new velocity of individuals is first computed by using Eq. (31). Then the new position of individuals is updated by using Eq. (33). A repair action as in Eq (44) is applied if the new created velocity and position of individuals violate their limits.

Step 5: Run the power flow using the newly generated population and calculate the fitness function (42) for the normal case, and fitness function (43) for the outage case.

Step 6: The second new population is created in this step, based on the first population created by the PGPSO mechanism, by using the mutation stage of DE as in Eq. (34). A repair action as in Eq (44) is applied if the new position violates its limits.

Step 7: The crossover stage of DE is applied to create new individuals from the second new created population using Eq. (35).

Step 8: Run the power flow using the new individuals generated from the crossover stage and calculate the fitness function (42) for the normal case, and fitness function (43) for the outage case.

Step 9: The best individuals are selected via the selection stage of DE for the next generation. The fitness values of individuals from the first generated populations are compared to those from the second generated populations. The new individual is selected by:

$$X_{id}^{new(k)} = \begin{cases} X_{id}^{''(k)} & \text{if } FT_d^{''(k)} \le FT_d^{(k)} \\ X_{id}^{(k)} & otherwise \end{cases} \tag{45}$$

Update the new individual $X_d^{new(k)}$ and the corresponding fitness value $FT_d^{new(d)}$ accordingly.

Step 10: The best population is updated in this step. The update of the best position of each individual is described as follows:

$$Pbest_d = \begin{cases} X_{id}^{new(k)} & \text{if } FT_d^{new(k)} \le FT_d^{best} \\ Pbest_d & otherwise \end{cases} \tag{46}$$

Update the corresponding better fitness function FT_d^{best}. Update $Pbest_d$ to *Gbest*.

Step 11: If the current iteration k is lower than the maximum iteration $Iter_{max}$, increase k and return step 4. Otherwise, stop.

6. Numerial results

The suggested PGPSO-DE has been tested on the IEEE 30-bus system for both the normal case and selected outage cases. The fuel cost function is considered with a quadratic function and a function with VPEs. The test system has six thermal generating units, four tap changing transformers, and 41 transmission lines. Besides, there are nine shunt power compensators at buses 10, 12, 15, 17, 20, 21, 23, 24 and 29. The data of the test system and the transmission line limits are from [6]. Table A.1 gives the generator data with the quadratic fuel cost function while Table A.2 gives the fuel cost coefficients for valve point loading effects. Table A.3 represents the limits for the bus voltage and transformer tap settings. Shunt power compensators have a lower limit of 0 MVar and an upper limit of 5 MVar. The power flow problem in this study is solved by the TDPF toolbox [35].

Table 1. Control parameters of PGPSO-DE for the TDOPF with normal and contingency cases

Parameters	$Iter_{max}$	N_p	c_1	c_2	R	F	CR
Case 1	150	10	2.05	2.05	0.15	0.7	0.5
Case 2	200	50	2.05	2.05	0.15	0.7	0.5
Case 3	250	10	2.05	2.05	0.15	0.7	0.5
Case 4	300	20	2.05	2.05	0.15	0.7	0.5

For implementing the proposed PGPSO-DE method to the TDOPF problem, its control parameters are selected for different cases of normal and contingency as shown in Table 1 as follows:
Case 1: Normal case with the quadratic objective function.
Case 2: Normal case with the objective function taking into account VPEs.
Case 3: Selected outage case with the quadratic objective function.
Case 4: Selected outage case with the objective function taking into account VPEs.
The code of the suggested PGPSO-DE method was written in Matlab software. To find the best solution, each case was run in 50 separate trials.

A. Normal case

The proposed PGPSO-DE approach is implemented to deal with the normal TDOPF problem. The objective function is taken into account the quadratic function and VPEs.

A.1. Quadratic objective function

To verify the effectiveness of the proposed PGPSO-DE method, it is firstly tested on the IEEE 30-bus system to solve the conventional OPF problem with the quadratic objective function. For this case, the number of individuals N_p of PGPSO-DE is set to 50 for fair appraisal since most compared algorithms also set this parameter to 50. The fuel costs obtained from PGPSO-DE including minimum, average and maximum values are compared to those from other optimization algorithms as shown in Table 2. It can be seen that the minimum fuel cost of PGPSO-DE is better than other compared methods and close to GWO [14] and IKHA [16]. In addition, the average fuel cost of PGPSO-DE is the best value among compared methods and the standard deviation is rather small. Hence, the proposed method provides a very high and robustness solution quality in this case. It is further confirmed as seen from Figure 2 which shows the algorithm's robustness for 50 independent runs. Figure 3 shows the convergence characteristic of PGPSO-DE for the IEEE 30 bus test system with the conventional OPF problem. The minimum fuel cost achieved by the PGPSO-DE method is 800.4141 ($/h).

Table 2. Result comparison for the IEEE 30 bus test system with the conventional OPF problem

Algorithms	Minimum Fuel cost ($/h)	Average Fuel cost ($/h)	Maximum Fuel cost ($/h)	Standard deviation	Parameters Setting	
					N_p	$Iter_{max}$
ABC [12]	800.6600	800.8715	801.8674	-	50	200
ARCBBO [13]	800.5159	800.6412	800.9262	-	50	200
GWO [14]	801.413	801.655	801.958	0.1129	-	300
MSA [15]	800.5099	-	-	-	50	100
IKHA [16]	800.4143	-	-	-	30	500
IMFO [17]	800.3848*	-	-	-	50	500
GABC [27]	800.4401	800.6390	800.7959	1.58142	50	100
CWOA [28]	800.1998*	-	-	-	50	100
PGPSO-DE	800.4141	800.5708	802.8181	0.3978	50	150

*Violated solution

To investigate the effect of temperature, the TDOPF problem is performed with each value of temperature rise ($T_{RatedRise}$). The base temperature (T_{Base}) is selected as 100 ºC. The ambient temperature (T_{Amp}) and the reference temperature (T_{Ref}) are selected as 25 ºC. The temperature constant (T_F) is 228.1 ºC because all conductors are considered hard-drawn aluminium [1]. For a fair comparison with GABC [27], the upper voltage limit of load bus, in this case, is set to 1.06 p.u. as the same in [27]. Table 3 presents the minimum fuel cost and the power loss obtained by the proposed PGPSO-DE method corresponding to each value of $T_{RatedRise}$ for the IEEE 30 bus test system. It can be observed that PGPSO-DE offers a better solution than GABC [27] and

CWOA [28]. For 0 ºC temperature rise, the fuel cost and the real power loss obtained by PGPSO-DE are 799.8667 ($/h) and 8.8670 MW, respectively. These values become 802.9909 ($/h) and 9.4663 MW, respectively, for 100 ºC temperature rise. For the 30 ºC temperature rise, the increase in fuel cost and power loss are 0.14% and 2.61%, respectively. Figure 4 depicts the effect of temperature rise on fuel cost and power loss. When the temperature rise ($T_{RatedRise}$) increases, the fuel cost and power loss also increase. In general, the fuel cost increase by 0.04% approximately for every 10 ºC temperature rise. Figure 5 depicts the convergence characteristic of PGPSO-DE for the IEEE 30 bus system with the quadratic objective function corresponding to $T_{RatedRise}$ = 30 ºC. It can be observed that the objective function converges smoothly to the near optimal solution.

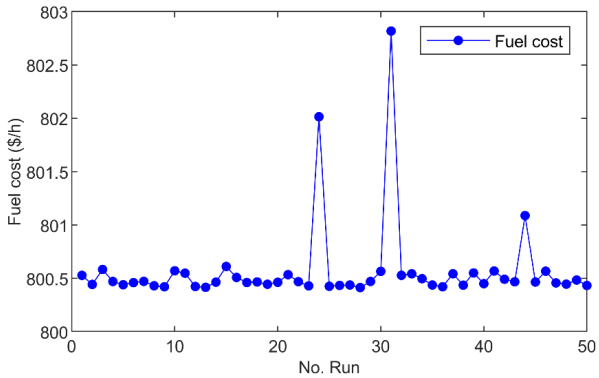

Figure 2. Fuel cost of fifty independent runs for the conventional OPF problem for the IEEE 30 bus system

Table 3. Fuel cost and power loss obtained for the TDOPF problem with the quadratic objective function

	Fuel cost ($/h)			Power loss (MW)		
$T_{RatedRise}$	GABC [27]	CWOA [28]	PGPSO-DE	GABC [27]	CWOA [28]	PGPSO-DE
0	800.0627	800.0227	799.8667	8.912071	8.7731	8.8670
10	800.4531	800.4010	800.2735	9.029315	8.9258	8.9716
20	800.8292	800.7836	800.6067	9.142254	9.0924	9.0335
30	801.1922	801.1336	801.012	9.251205	9.1346	9.1047
40	801.5429	801.4729	801.3203	9.356453	9.2749	9.1788
50	801.8822	801.8016	801.6144	9.458257	9.3417	9.1934
60	802.2109	802.1204	801.941	9.556852	9.4663	9.2650
70	802.5297	802.4294	802.1624	9.652453	9.5133	9.3602
80	802.8392	802.7296	802.4328	9.745256	9.6674	9.3678
90	803.14	803.0297	802.7393	9.83544	9.7513	9.4046
100	803.4327	803.3224	802.9909	9.923173	9.8017	9.4663

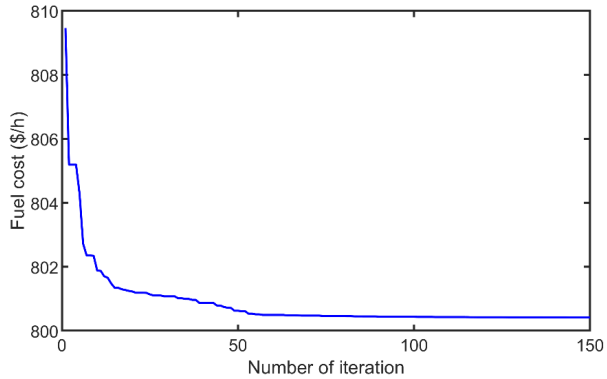

Figure 3. Convergence characteristic of PGPSO-DE for the IEEE 30 bus system with the conventional OPF problem.

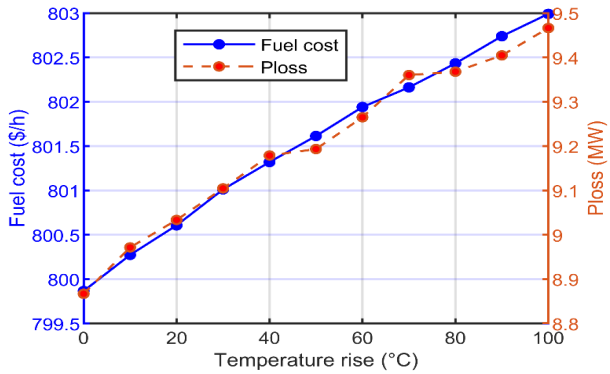

Figure 4. Temperature rise effect on fuel cost and power loss for the TDOPPF problem with the quadratic objective function.

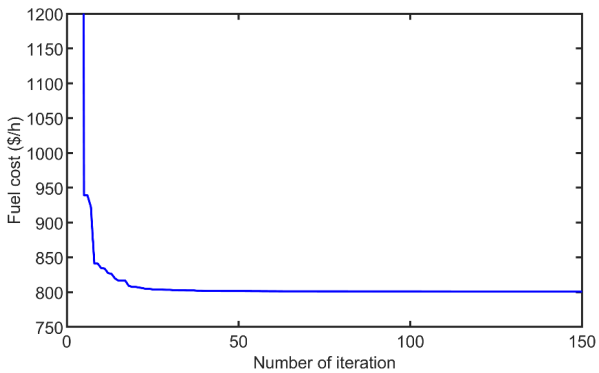

Figure 5. Convergence characteristic of PGPSO-DE for the TDOPF problem with the quadratic objective function corresponding to $T_{RatedRise}$ = 30 ºC.

A.2. Objective function considering VPEs.

The valve point loading effects is taken into account in the objective function of the TDOPF problem in this case. Table 4 shows the obtained results of fuel cost and power loss for the rise in temperature for the TDOPF problem with VPEs. For 0 ºC temperature rise, the fuel cost obtained by the PGPSO-DE method is 919.825 ($/h) and the real power loss is 9.8902 MW. For 30 ºC temperature rise, the increase in fuel cost is 0.22% and 4.12 % for power loss. The obtained fuel cost becomes 925.5945 ($/h) and the real power loss is 11.3242 MW when the temperature rise

$T_{RatedRise}$ is 100 ºC. Figure 6 illustrates the effect of temperature rise on fuel cost and power loss for the IEEE 30 bus system with valve point loading effects. The general trend is for increasing fuel cost and power loss as the temperature rises. Figure 7 shows the convergence characteristic of PGPSO-DE for the IEEE 30 bus system with the valve point loading effects for $T_{RatedRise}$ = 30 ºC. It can be observed that the objective function converges to the near-optimal solution after 150 iterations.

Table 4. Fuel cost and power loss obtained for the TDOPF problem with VPEs

$T_{RatedRise}$	Fuel cost ($/h)	Power loss (MW)
0	919.8525	9.8902
10	920.7833	10.0651
20	920.8674	10.1003
30	921.8648	10.3154
40	922.9310	10.4745
50	922.9798	10.6180
60	923.5945	10.7661
70	923.6734	10.8103
80	924.4393	11.0610
90	924.5678	11.1348
100	925.0736	11.3242

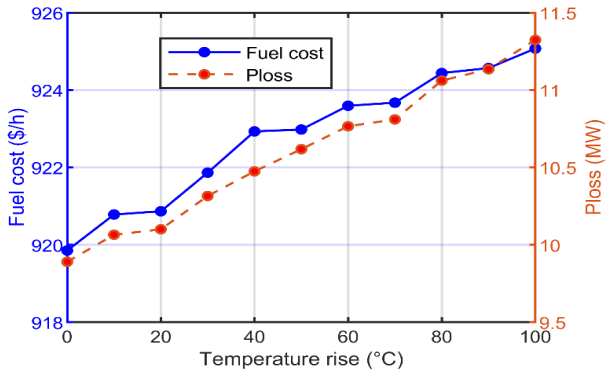

Figure 6. Temperature rise effect on fuel cost and power loss for the TDOPF problem with VPEs.

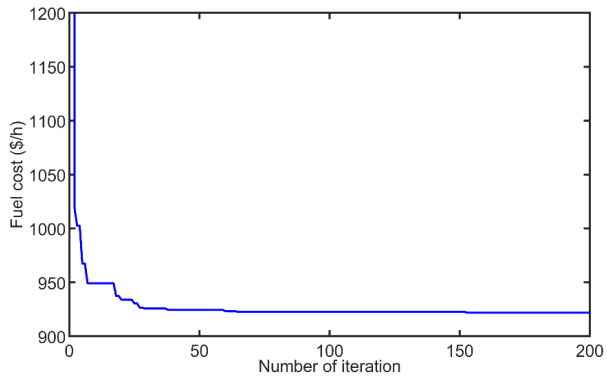

Figure 7. Convergence characteristic of PGPSO-DE for the IEEE 30 bus system with VPEs corresponding to $T_{RatedRise}$ = 30 ºC

B. Outage cases

To consider the outage of the transmission line, contingency analysis is carried out before solving the SC-TDOPF problem. The SI value is determined for each *N*-1 outage line.

Table 5. Contingency analysis of the IEEE 30 bus system

Outage line	Overload line	Line flow (MVA)	Line flow limit (MVA)	Overload rate (%)	Severity index
1-2	2	307.0136	130	236.1643	16.3035
	4	281.3522	130	216.4248	
	7	178.4014	90	198.2238	
	10	46.5144	32	145.3575	
1-3	1	274.0264	130	210.7895	9.4474
	3	86.1203	65	132.4928	
	6	92.7203	65	142.6466	
	10	35.2567	32	110.1773	
3-4	1	271.0750	130	208.5192	9.2390
	3	84.8816	65	130.5871	
	6	91.7672	65	141.1803	
	10	34.9449	32	109.2027	
2-5	1	165.4421	130	127.2632	8.5614
	3	74.6652	65	114.8695	
	6	102.9619	65	158.4030	
	7	123.6755	90	137.4172	
	10	35.4150	32	110.6719	
4-6	1	200.5759	130	154.2892	5.7600
	6	98.5645	65	151.6377	
	15	67.5536	65	103.9286	

The IEEE 30-bus system has 41 transmission lines, thus, there are 41 obtained SI values. The severe cases with the highest SI values will be selected as outage cases for the SC-TDOPF problem. In this study, five transmission lines 1-2, 1-3, 3-4, 2-5 and 4-6 are determined as severe cases since their SI values are higher than the other transmission lines. The contingency analysis of these five outage cases is given in Table 5, where each of the severe cases is considered in one outage case.The obtained results for both cases with a quadratic objective function and a function of VPEs are reported in the following subsections:

B.1. Quadratic objective function

For the SC-TDOPF problem with the quadratic function, the fuel cost and real power loss obtained by the proposed PGPSO-DE method corresponding to each value of $T_{RatedRise}$ are presented in Table 6 for the outage lines 1-2, 1-3, and 3-4, and in Table 7 for the outage lines 2-5 and 4-6. For 0 ^{o}C temperature rise, the proposed PGPSO-DE method provides the minimum fuel costs for outage lines 1-2, 1-3, 3-4, 2-5, and 4-6 are 823.7949 ($/h), 820.4042 ($/h), 819.5505 ($/h), 806.5713 ($/h), and 801.4946 ($/h), respectively. These values, in order, become 828.0905 ($/h), 823.3478 ($/h), 822.6376 ($/h), 808.7184 ($/h), and 804.1846 ($/h) for 100^{o}C temperature rise. For the real power loss, the proposed PGPSO-DE method provides the values of 6.1357 MW, 6.3038 MW, 6.6004 MW, 7.4138 MW, and 8.3652 MW for 0^{o}C temperature rise, and 6.3978 MW, 6.6481 MW, 7.2708 MW, 7.9547 MW, and 9.1687 for 100^{o}C temperature rise corresponding to the outage lines 1-2, 1-3, 3-4, 2-5, and 4-6. For 30^{o}C temperature rise, the increase in fuel cost and real power loss are 0.17% and 0.46 % for outage line 1-2, 0.11 % and 1.81% for outage line 1-3, 0.13 % and 2.49% for outage line 1-3, 0.1 % and 2.28% for outage line 2-5, and 0.12 % and 3.58% for outage line 4-6, respectively. Figure 8 shows the effect of temperature rise on fuel cost and power loss for the SC-TDOPF problem with the quadratic objective function. It can be seen that the fuel cost and power loss increase following the increase of $T_{RatedRise}$. Figure 9 depicts the convergence characteristic of PGPSO-DE for outage lines 1-2, 1-

3, 3-4, 2-5, and 4-6 for $T_{RatedRise}$ = 30 ºC. The convergence characteristics yielded by the proposed method for those cases are found to be stable. The optimal solution obtained by the proposed method is given in Appendix.

Table 6. Fuel cost and power loss obtained for the SC-TDOPF problem with quadratic objective function for outage lines 1-2, 1-3, and 3-4.

Outage case	Line 1-2		Line 1-3		Line 3-4	
$T_{RatedRise}$	Fuel cost ($/h)	Power loss (MW)	Fuel cost ($/h)	Power loss (MW)	Fuel cost ($/h)	Power loss (MW)
0	823.7949	6.1357	820.4042	6.3038	819.5505	6.6004
10	824.4885	6.2004	821.0448	6.4217	819.8601	6.6526
20	824.9029	6.2339	821.1104	6.3891	820.2708	6.7493
30	825.2031	6.1641	821.3032	6.4199	820.6233	6.7688
40	825.6662	6.2837	821.8879	6.4684	820.8518	6.7809
50	826.0028	6.2699	822.1185	6.5183	821.1988	7.0280
60	826.5077	6.3237	822.3815	6.5540	821.5800	6.9197
70	826.9197	6.3724	822.4503	6.4644	821.9318	6.9503
80	827.3582	6.2803	822.5881	6.5298	822.0921	6.9387
90	827.6874	6.2975	822.9092	6.6259	822.5010	7.0695
100	828.0905	6.3978	823.3478	6.6481	822.6376	7.2708

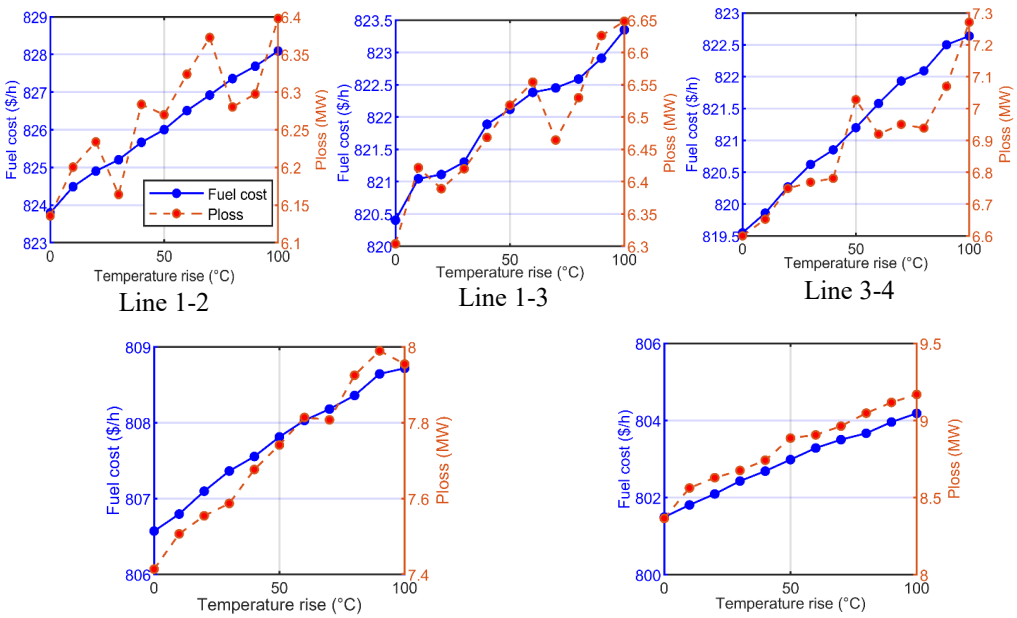

Figure 8. Temperature rise effect on fuel cost and power loss for the SC-TDOPPF problem with the quadratic objective function.

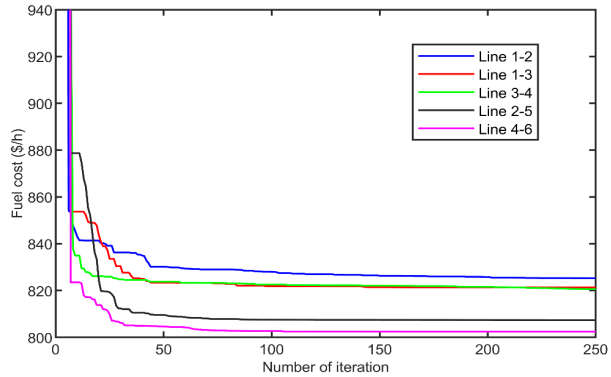

Figure 9. Convergence characteristic of PGPSO-DE for the SC-TDOPF problem with the quadratic objective function corresponding to $T_{RatedRise}$ = 30 ºC.

Table 7. Fuel cost and power loss obtained for the SC-TDOPF problem with quadratic objective function for outage lines 2-5 and 4-6.

Outage case	Line 2-5		Line 4-6	
$T_{RatedRise}$	Fuel cost ($/h)	Power loss (MW)	Fuel cost ($/h)	Power loss (MW)
0	806.5713	7.4138	801.4946	8.3652
10	806.7956	7.5068	801.8090	8.5623
20	807.0974	7.5545	802.0934	8.6289
30	807.3633	7.5871	802.4289	8.6759
40	807.5542	7.6766	802.6870	8.7421
50	807.8132	7.7412	802.9846	8.8857
60	808.0300	7.8139	803.2857	8.9063
70	808.1800	7.8076	803.5020	8.9634
80	808.3591	7.9252	803.6682	9.0475
90	808.6439	7.9897	803.9590	9.1169
100	808.7184	7.9547	804.1846	9.1687

B.2. Objective function considering VPEs.

In this case of the SC-TDOPF problem, the objective function comprises VPEs, which makes the SC-TDOPD becomes a non-convex optimization problem. Table 8 tabulates the fuel cost and power loss corresponding to each value of $T_{RatedRise}$ for the outage lines 1-2, 1-3, and 3-4. Similarly, Table 9 presents the obtained results for the outage lines 2-5 and 4-6. The fuel costs obtained by PGPSO-DE for 0ºC temperature rise are 1034.8118 ($/h), 1030.2897 ($/h), 1025.6910 ($/h), 962.5737 ($/h), 952.1968 ($/h) for outage lines 1-2, 1-3, 3-4, 2-5, and 4-6, respectively. These values are 1035.8552 ($/h), 1034.2135 ($/h), 1030.9578 ($/h), 961.7055 ($/h), and 954.3138 ($/h) for 100ºC temperature rise. For 30ºC temperature rise, the increases in fuel cost are 0.05%, 0.16%, 0.18%, 0.03%, and 0.09% for outage lines 1-2, 1-3, 3-4, 2-5, and 4-6, respectively.

Regarding the real power loss, for 0ºC temperature rise, PGPSO-DE achieves the values of 5.3209 MW, 5.9945 MW, 6.3729 MW, 8.0992 MW, and 8.3652 MW for the outage lines 1-2, 1-3, 3-4, 2-5, and 4-6. For 100ºC temperature rise, the values of power loss become 5.5706 MW, 6.3244 MW, for 6.8565 MW, 8.7871 MW, and 7.8437 corresponding to the outage lines 1-2, 1-3, 3-4, 2-5, and 4-6. For 30ºC temperature rise, the increases in power loss are 1.63%, 2.47%, 2.90%, 2.14%, and 2.82% for corresponding outage lines.

Figure 10 shows the effect of temperature rise on fuel cost and power loss for the SC-TDOPF problem with valve point loading effects for outage lines 1-2, 1-3, 3-4, 2-5, and 4-6. It can be seen that the fuel cost and power loss increase with the increase of $T_{RatedRise}$. Figure 11 illustrates the convergence characteristic of PGPSO-DE for outage cases for $T_{RatedRise}$ = 30ºC. It can be observed

that the proposed method converges smoothly to the near-optimal solution for outage lines 1-2, 1-3, 3-4, 2-5, and 4-6. The optimal solution obtained by PGSO-DE for this case is given in

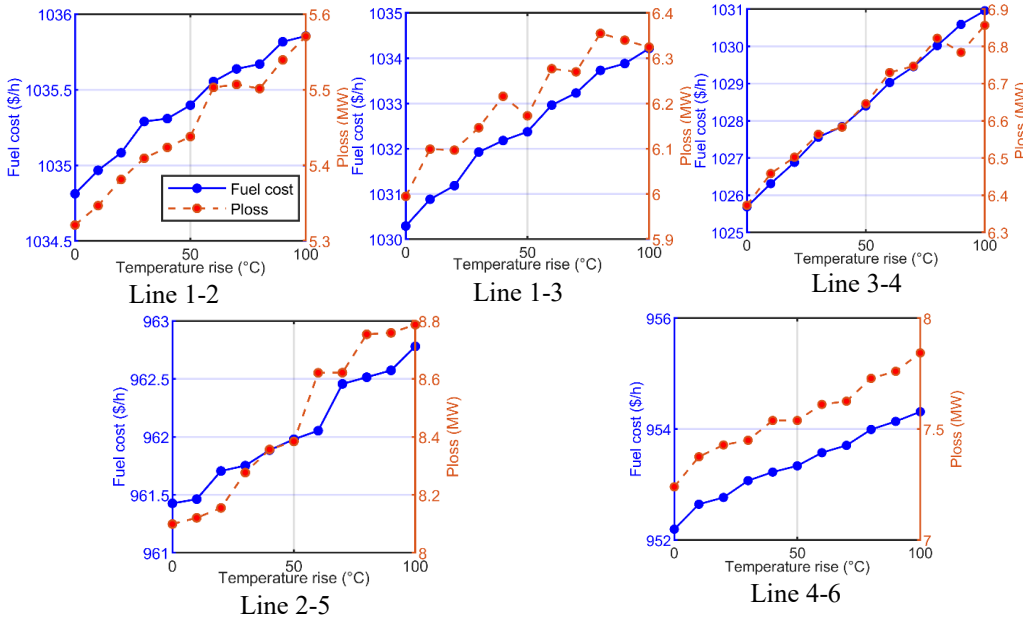

Figure 10. Temperature rise effect on fuel cost and power loss for the SC-TDOPPF problem with VPEs.

Appendix.

Table 8. Fuel cost and power loss obtained for the SC-TDOPF problem with VPEs for outage lines 1-2, 1-3, and 3-4.

Outage case	Line 1-2		Line 1-3		Line 3-4	
$T_{RatedRise}$	Fuel cost ($/h)	Power loss (MW)	Fuel cost ($/h)	Power loss (MW)	Fuel cost ($/h)	Power loss (MW)
0	1034.8118	5.3209	1030.2897	5.9945	1025.6910	6.3729
10	1034.9668	5.3466	1030.8810	6.0989	1026.3124	6.4584
20	1035.0830	5.3813	1031.1819	6.0967	1026.8841	6.5023
30	1035.2897	5.4093	1031.9249	6.1463	1027.5598	6.5637
40	1035.3090	5.4237	1032.1796	6.2157	1027.8454	6.5829
50	1035.3977	5.4380	1032.3729	6.1726	1028.4009	6.6460
60	1035.5541	5.5031	1032.9630	6.2767	1029.0285	6.7297
70	1035.6378	5.5070	1033.2300	6.2698	1029.4535	6.7469
80	1035.6697	5.5015	1033.7299	6.3547	1030.0198	6.8218
90	1035.8174	5.5395	1033.8801	6.3397	1030.5906	6.7837
100	1035.8552	5.5706	1034.2135	6.3244	1030.9578	6.8565

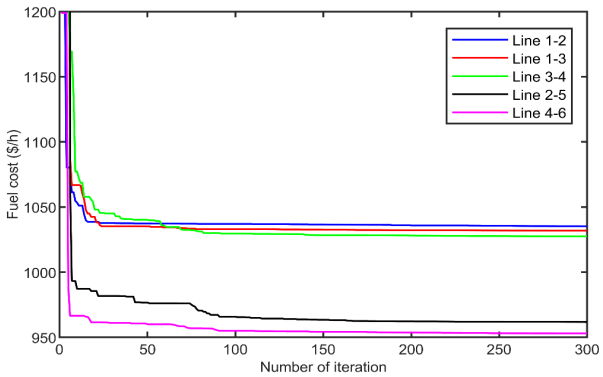

Figure 11. Convergence characteristic of PGPSO-DE for the SC-TDOPF problem with the VPEs corresponding to $T_{RatedRise}$ = 30 ºC.

Table 9. Fuel cost and power loss obtained for the SC-TDOPF problem with VPEs for outage lines 2-5 and 4-6.

Outage case	Line 2-5		Line 4-6	
$T_{RatedRise}$	Fuel cost ($/h)	Power loss (MW)	Fuel cost ($/h)	Power loss (MW)
0	961.4261	8.0992	952.1968	7.2400
10	961.4625	8.1205	952.6466	7.3755
20	961.7055	8.1547	952.7685	7.4288
30	961.7517	8.2767	953.0724	7.4499
40	961.8854	8.3563	953.2266	7.5389
50	961.9792	8.3842	953.3388	7.5391
60	962.0529	8.6210	953.5756	7.6115
70	962.4567	8.6214	953.7074	7.6258
80	962.5144	8.7538	953.9941	7.7289
90	962.5737	8.7589	954.1395	7.7605
100	962.7802	8.7871	954.3138	7.8437

7. Conclusion

This study has investigated the OPF problem considering the temperature effect. The objective function has been examined with the quadratic cost function and a function comprising of VPEs. In addition, the security constraint has also been considered for the OPF problem. Considering the temperature effect increases the accuracy of the OPF problem. The SC-TDOPF is a non-linear, non-convex, and large-scale problem which is a real challenge for solution methods. In this paper, the proposed PGPSO-DE method has been successfully dealt with the considered SC-TDOPF problem. The proposed method has been tested on the IEEE 30-bus system with normal and outage cases for objective functions of quadratic and valve point effects. The obtained results have shown that the proposed method is effective in dealing with the SC-TDOPF problem with quadratic and VPEs of fuel cost function. As a result, the suggested PGPSO-DE method could be a favourable method for dealing with the large-scale and difficult optimization problems in power systems. The large-scale test systems and other complex objective functions would be examined in future works for the TDOPF problem.

8. Acknowledgments

This research is funded by Vietnam National University HoChiMinh City (VNU-HCM) under grant number **C2021-20-14**.

9. Appendix

Table A.1. Cost coefficients of thermal units with with a quadratic cost function in the IEEE-bus system

Unit	$P_{i,max}$ (MW)	$P_{i,min}$ (MW)	$Q_{i,max}$ (MVAr)	$Q_{i,min}$ (MVAr)	Cost coefficients		
					a_i (\$/h)	b_i (\$/MWh)	c_i (\$/MW^{2}h)
1	200	50	200	-20	0	2.00	0.00375
2	80	20	100	-20	0	1.75	0.01750
5	50	15	80	-15	0	1.00	0.06250
8	35	10	60	-15	0	3.25	0.00834
11	30	10	50	-10	0	3.00	0.02500
13	40	12	60	-15	0	3.00	0.02500

Table A.2. Cost coefficients of of thermal units with VPEs in the IEEE 30-bus system

Unit	$P_{i,max}$ (MW)	$P_{i,min}$ (MW)	Cost coefficients				
			a_i (\$/h)	b_i (\$/MWh)	c_i (\$/MW^{2}h)	e_i (\$/h)	f_i (1/MW)
1	200	50	150	2.00	0.00160	50	0.063
2	80	20	25	2.50	0.01000	40	0.098
5	50	15	0	1.00	0.06250	0	0
8	35	10	0	3.25	0.00834	0	0
11	30	10	0	3.00	0.02500	0	0
13	40	12	0	3.00	0.02500	0	0

Table A.3. Limits transformer tap setting and bus voltage for the IEEE 30-bus system

	Lower limit (p.u.)	Upper limit (p.u.)
Transformer tap setting (T_k)	0.90	1.10
Slack bus voltage (V_{g1})	0.90	1.10
Generator bus voltage (V_{gi})	0.90	1.10
Load bus voltage (V_{li})	0.95	1.05

Table A.4. Optimal solutions by HPSO-DE for TDOPD problem (Normal and Outage cases) with quadratic fuel cost function corresponding to $T_{RatedRise}$ = 30 °C

Optimal solution	Normal case	Outage line 1-2	Outage line 1-3	Outage line 3-4	Outage line 2-5	Outage line 4-6
P_{G1} (MW)	176.3517	122.8073	127.3085	129.4705	157.0478	169.3141
P_{G2} (MW)	48.8281	62.7836	61.2513	60.7798	42.4111	47.1001
P_{G5} (MW)	21.7061	25.6834	24.4011	25.3942	24.9709	21.6438
P_{G8} (MW)	21.5351	35.0000	35.0000	34.8064	34.5102	28.6375
P_{G11} (MW)	12.0837	22.0504	21.1753	20.3922	17.1942	13.3805
P_{G13} (MW)	12.0000	21.2393	20.6837	19.3256	14.8529	12.0000
V_{G1} (p.u.)	1.0945	1.0740	1.0802	1.0494	1.0770	1.0860
V_{G2} (p.u.)	1.0746	1.0556	1.0581	1.0292	1.0587	1.0669
V_{G5} (p.u.)	1.0429	1.0287	1.0282	1.0048	1.0244	1.0389
V_{G8} (p.u.)	1.0469	1.0390	1.0368	1.0128	1.0334	1.0394
V_{G11} (p.u.)	1.0465	1.0830	1.1000	1.0819	1.0630	1.0813
V_{G13} (p.u.)	1.0561	1.0656	1.0480	1.0533	1.0735	1.0376
Q_{C10} (MVAr)	5.0000	0.0000	1.9495	0.0146	0.1535	3.7475
Q_{C12} (MVAr)	2.1018	0.0000	2.5254	1.7606	4.1345	0.8124
Q_{C15} (MVAr)	3.9448	3.5929	2.3804	3.0843	0.1873	1.9432
Q_{C17} (MVAr)	5.0000	4.6862	4.5985	5.0000	1.9768	5.0000
Q_{C20} (MVAr)	3.2950	3.8692	4.5061	3.8157	4.1076	0.0019
Q_{C21} (MVAr)	4.9877	2.6067	0.4104	4.9866	4.2745	5.0000

Optimal solution	Normal case	Outage line 1-2	Outage line 1-3	Outage line 3-4	Outage line 2-5	Outage line 4-6
Q_{C23} (MVAr)	5.0000	4.0042	4.2849	1.4906	4.2358	4.1888
Q_{C24} (MVAr)	5.0000	1.7054	5.0000	5.0000	5.0000	5.0000
Q_{C29} (MVAr)	5.0000	2.6949	1.5807	0.2004	1.4451	4.1379
T_{11} (p.u.)	1.0574	1.0014	1.0811	1.0119	1.0436	1.0610
T_{12} (p.u.)	0.9000	0.9916	0.9227	0.9361	0.9031	0.9384
T_{15} (p.u.)	0.9713	0.9958	0.9683	1.0093	1.0099	0.9450
T36 (p.u.)	0.9875	0.9740	0.9724	0.9621	0.9778	0.9949

Table A.5. Optimal solutions by HPSO-DE for TDOPD problem (Normal and Outage cases) with VPEs corresponding to $T_{RatedRise}$ = 30 ºC

Optimal solution	Normal case	Outage line 1-2	Outage line 1-3	Outage line 3-4	Outage line 2-5	Outage line 4-6
P_{G1} (MW)	149.7332	99.8696	127.5941	129.8608	149.7352	149.7283
P_{G2} (MW)	52.0594	80.0000	52.0571	52.0565	51.2808	52.0546
P_{G5} (MW)	22.3130	26.8057	27.6889	26.7472	27.1427	24.3538
P_{G8} (MW)	33.2914	35.0000	35.0000	35.0000	35.0000	31.7920
P_{G11} (MW)	16.6501	24.4057	25.4596	23.6783	16.6122	16.4309
P_{G13} (MW)	17.0357	22.7283	21.7466	22.6209	12.0004	16.4903
V_{G1} (p.u.)	1.0694	1.0706	1.0809	1.0492	1.0848	1.0727
V_{G2} (p.u.)	1.0492	1.0596	1.0580	1.0262	1.0577	1.0576
V_{G5} (p.u.)	1.0137	1.0307	1.0278	1.0020	0.9906	1.0327
V_{G8} (p.u.)	1.0337	1.0408	1.0285	1.0091	1.0261	1.0429
V_{G11} (p.u.)	1.0827	1.0964	1.0767	1.0759	0.9919	1.0935
V_{G13} (p.u.)	1.0781	1.0428	1.0641	1.0677	1.1000	1.0469
Q_{C10} (MVAr)	1.4073	2.7162	5.0000	2.9103	5.0000	2.6873
Q_{C12} (MVAr)	0.4978	3.2551	0.0469	2.3769	1.1882	3.2422
Q_{C15} (MVAr)	2.2904	4.9133	4.3504	3.1394	2.0455	3.6043
Q_{C17} (MVAr)	2.6629	4.5545	4.2242	2.6968	5.0000	4.0109
Q_{C20} (MVAr)	1.0981	2.2348	4.9931	3.2844	5.0000	4.9691
Q_{C21} (MVAr)	4.7504	4.6913	0.0358	3.6180	3.9394	3.0023
Q_{C23} (MVAr)	2.8429	5.0000	0.6435	0.0036	2.4749	4.9121
Q_{C24} (MVAr)	3.8930	2.7292	5.0000	5.0000	2.7409	4.0099
Q_{C29} (MVAr)	3.4787	2.7533	2.5568	3.0209	2.3062	2.5498
T_{11} (p.u.)	1.0318	1.0837	0.9922	0.9493	1.0928	1.0135
T_{12} (p.u.)	0.9000	0.9114	0.9887	1.0368	1.0277	1.0067
T_{15} (p.u.)	1.0812	0.9761	0.9989	0.9857	1.0035	0.9791
T36 (p.u.)	0.9690	0.9747	0.9684	0.9673	1.0316	0.9812

10. References

[1]. S. Frank, J. Sexauer, and S. Mohagheghi, "Temperature-Dependent Power Flow," *IEEE Transactions on Power Systems,* vol. 28, no. 4, pp. 4007-4018, 2013.

[2]. B. Wollenberg and A. Wood, "Power generation, operation and control," *Ed. John Wiley & Sons, USA,* 1996.

[3]. S. Frank, I. Steponavice, and S. Rebennack, "Optimal power flow: a bibliographic survey I," *Energy Systems,* vol. 3, no. 3, pp. 221-258, 2012/09/01 2012.

[4]. D. I. Sun, B. Ashley, B. Brewer, A. Hughes, and W. F. Tinney, "Optimal Power Flow By Newton Approach," *IEEE Transactions on Power Apparatus and Systems,* vol. PAS-103, no. 10, pp. 2864-2880, 1984.

[5]. R. Mota-Palomino and V. H. Quintana, "Sparse Reactive Power Scheduling by a Penalty Function - Linear Programming Technique," *IEEE Transactions on Power Systems,* vol. 1, no. 3, pp. 31-39, 1986.
[6]. O. Alsac and B. Stott, "Optimal Load Flow with Steady-State Security," *IEEE Transactions on Power Apparatus and Systems,* vol. PAS-93, no. 3, pp. 745-751, 1974.
[7]. R. C. Burchett, H. H. Happ, and D. R. Vierath, "Quadratically Convergent Optimal Power Flow," *IEEE Transactions on Power Apparatus and Systems,* vol. PAS-103, no. 11, pp. 3267-3275, 1984.
[8]. Y. Xihui and V. H. Quintana, "Improving an interior-point-based OPF by dynamic adjustments of step sizes and tolerances," *IEEE Transactions on Power Systems,* vol. 14, no. 2, pp. 709-717, 1999.
[9]. M. Todorovski and D. Rajicic, "An initialization procedure in solving optimal power flow by genetic algorithm," *IEEE Transactions on Power Systems,* vol. 21, no. 2, pp. 480-487, 2006.
[10]. M. A. Abido, "Optimal power flow using particle swarm optimization," *International Journal of Electrical Power & Energy Systems,* vol. 24, no. 7, pp. 563-571, 2002/10/01/ 2002.
[11]. A. Abou El Ela, M. Abido, and S. J. E. P. S. R. Spea, "Optimal power flow using differential evolution algorithm," vol. 80, no. 7, pp. 878-885, 2010.
[12]. M. Rezaei Adaryani and A. Karami, "Artificial bee colony algorithm for solving multi-objective optimal power flow problem," *International Journal of Electrical Power & Energy Systems,* vol. 53, pp. 219-230, 2013/12/01/ 2013.
[13]. A. Ramesh Kumar and L. Premalatha, "Optimal power flow for a deregulated power system using adaptive real coded biogeography-based optimization," *International Journal of Electrical Power & Energy Systems,* vol. 73, pp. 393-399, 2015/12/01/ 2015.
[14]. A. A. El-Fergany and H. M. Hasanien, "Single and Multi-objective Optimal Power Flow Using Grey Wolf Optimizer and Differential Evolution Algorithms," *Electric Power Components and Systems,* vol. 43, no. 13, pp. 1548-1559, 2015/08/09 2015.
[15]. A.-A. A. Mohamed, Y. S. Mohamed, A. A. M. El-Gaafary, and A. M. Hemeida, "Optimal power flow using moth swarm algorithm," *Electric Power Systems Research,* vol. 142, pp. 190-206, 2017/01/01/ 2017.
[16]. G. Chen, Z. Lu, and Z. Zhang, "Improved Krill Herd Algorithm with Novel Constraint Handling Method for Solving Optimal Power Flow Problems," *Energies,* vol. 11, no. 1, 2018.
[17]. M. A. Taher, S. Kamel, F. Jurado, and M. Ebeed, "An improved moth-flame optimization algorithm for solving optimal power flow problem," *International Transactions on Electrical Energy Systems,* https://doi.org/10.1002/etep.2743 vol. 29, no. 3, p. e2743, 2019/03/01 2019.
[18]. T. Niknam, M. R. Narimani, and R. Azizipanah-Abarghooee, "A new hybrid algorithm for optimal power flow considering prohibited zones and valve point effect," *Energy Conversion and Management,* vol. 58, pp. 197-206, 2012/06/01/ 2012.
[19]. M. Ghasemi, S. Ghavidel, S. Rahmani, A. Roosta, and H. Falah, "A novel hybrid algorithm of imperialist competitive algorithm and teaching learning algorithm for optimal power flow problem with non-smooth cost functions," *Engineering Applications of Artificial Intelligence,* vol. 29, pp. 54-69, 2014/03/01/ 2014.
[20]. J. Radosavljević, D. Klimenta, M. Jevtić, and N. Arsić, "Optimal Power Flow Using a Hybrid Optimization Algorithm of Particle Swarm Optimization and Gravitational Search Algorithm," *Electric Power Components and Systems,* vol. 43, no. 17, pp. 1958-1970, 2015/10/21 2015.
[21]. A. Panda and M. Tripathy, "Security constrained optimal power flow solution of wind-thermal generation system using modified bacteria foraging algorithm," *Energy,* vol. 93, pp. 816-827, 2015/12/15/ 2015.

[22]. Y. Xu, H. Yang, R. Zhang, Z. Y. Dong, M. Lai, and K. P. Wong, "A contingency partitioning approach for preventive-corrective security-constrained optimal power flow computation," *Electric Power Systems Research,* vol. 132, pp. 132-140, 2016/03/01/ 2016.
[23]. K. Pandiarajan and C. K. Babulal, "Fuzzy harmony search algorithm based optimal power flow for power system security enhancement," *International Journal of Electrical Power & Energy Systems,* vol. 78, pp. 72-79, 2016/06/01/ 2016.
[24]. B. Mahdad and K. Srairi, "Security constrained optimal power flow solution using new adaptive partitioning flower pollination algorithm," *Applied Soft Computing,* vol. 46, pp. 501-522, 2016/09/01/ 2016.
[25]. L. d. M. Carvalho, A. M. L. d. Silva, and V. Miranda, "Security-Constrained Optimal Power Flow via Cross-Entropy Method," *IEEE Transactions on Power Systems,* vol. 33, no. 6, pp. 6621-6629, 2018.
[26]. C. G. Marcelino *et al.*, "Solving security constrained optimal power flow problems: a hybrid evolutionary approach," *Applied Intelligence,* vol. 48, no. 10, pp. 3672-3690, 2018/10/01 2018.
[27]. H. T. Jadhav and P. D. Bamane, "Temperature dependent optimal power flow using g-best guided artificial bee colony algorithm," *International Journal of Electrical Power & Energy Systems,* vol. 77, pp. 77-90, 2016/05/01/ 2016.
[28]. D. Prasad, A. Mukherjee, and V. Mukherjee, "Temperature dependent optimal power flow using chaotic whale optimization algorithm," *Expert Systems,* https://doi.org/10.1111/exsy.12685 vol. 38, no. 4, p. e12685, 2021/06/01 2021.
[29]. P. M. Le, T. L. Duong, D. N. Vo, T. T. Le, S. Q. J. I. J. o. E. E. Nguyen, and Informatics, "An Efficient Hybrid Method for Solving Security-Constrained Optimal Power Flow Problem," vol. 12, no. 4, pp. 933-955, 2020.
[30]. J. Kennedy and R. Eberhart, "Particle swarm optimization," in *Proceedings of ICNN'95-international conference on neural networks*, 1995, vol. 4, pp. 1942-1948: IEEE.
[31]. M. Clerc and J. Kennedy, "The particle swarm - explosion, stability, and convergence in a multidimensional complex space," *IEEE Transactions on Evolutionary Computation,* vol. 6, no. 1, pp. 58-73, 2002.
[32]. D. T. Pham and G. J. E. L. Jin, "Genetic algorithm using gradient-like reproduction operator," vol. 31, pp. 1558-1559, 1995.
[33]. J. Wen, Q. Wu, L. Jiang, and S. J. E. L. Cheng, "Pseudo-gradient based evolutionary programming," vol. 39, no. 7, pp. 631-632, 2003.

Minh-Trung Dao received a B.Sc. degree in Electrical Engineering from Can Tho University, Vietnam, in 2005 and M.Eng. degree in Electrical Engineering from University of Technology - Viet Nam National University Ho Chi Minh City in 2012. Since 2005, he has been with the Department of Electrical Engineering, Can Tho University in Can Tho city, Viet Nam, where he is currently a lecturer. His research interests include power system optimization, power system operation and control, power system analysis, and renewable energy systems. Now, he is also a PhD student at University of Technology - Viet Nam National University Ho Chi Minh City (from 8/2021).

Khoa Hoang Truong received his B.Eng. degree in electrical engineering from Ho Chi Minh City University of Technology, VNU-HCM, Vietnam, in 2012. He also received his MSc degree (Applied Sciences) and Ph.D. degree in Electrical and Electronics Engineering from Universiti Teknologi PETRONAS, Malaysia, in 2016 and 2020, respectively. He is currently a Lecturer at Department of Power Delivery, Faculty of Electrical and Electronics Engineering, Ho Chi Minh City University of Technology, VNU-HCM, Vietnam. His research interests are power system operation and control, distributed generation, microgrids, and artificial intelligence-based algorithms.

Duy-Phuong N. Do was born in Can Tho city, VietNam in 1982. He received B.S, M.Sc and Ph.D degree in electrical engineering from Can Tho University, Ho Chi Minh University of Technology, Vietnam and Gyeongsang National University, Korea in 2005, 2008 and 2017 respectively. His research interests include wind speed forecast, voltage stability evaluation of power system, and power loss minimization in distribution network.

Bao-Huy Truong received the B.Eng. degree in Electrical and Electronics Engineering from Ho Chi Minh City University of Technology (HCMUT), VNU-HCM, Vietnam, in 2017 and the M.S. degree in Electrical and Electronics Engineering from Universiti Teknologi PETRONAS (UTP), Malaysia, in 2020. He is currently a Research Officer with Institute of Engineering and Technology, Thu Dau Mot University, Binh Duong Province, Vietnam. His research interests are renewable energy power generation, artificial intelligence-based algorithms and their application in optimization problems.

Khai Phuc Nguyen received his B.Eng. and M.Eng. degrees from Ho Chi Minh City University of Technology, Vietnam, in 2010 and 2012, respectively, and his Ph.D. in electrical engineering from Shibaura Institute of Technology, Tokyo, Japan, in 2017. His research interests are Artificial Intelligence (AI) in power system optimization, operation and control, power system analysis, and automation in power systems.

Dieu Ngoc Vo received his B.Eng. and M.Eng. degrees in electrical engineering from Ho Chi Minh City University of Technology, Ho Chi Minh city, Vietnam, in 1995 and 2000, respectively and his D.Eng. degree in energy from Asian Institute of Technology (AIT), Pathumthani, Thailand in 2007. He is Research Associate at Energy Field of Study, AIT and Head of Department of Power Systems, Faculty of Electrical and Electronic Engineering, Ho Chi Minh City University of Technology, Ho Chi Minh city, Vietnam. His research interests are applications of AI in power system optimization, power system operation and control, power system analysis, and power systems under deregulation and restructuring.